Canadian Science Publishing
Canadian Journal of Fisheries and Aquatic Sciences
Journal canadien des sciences halieutiques et aquatiques

Accounting for Spatial Complexities in the Calculation of Biological Reference Points: Effects of Misdiagnosing Population Structure for Stock Status Indicators

Journal:	*Canadian Journal of Fisheries and Aquatic Sciences*
Manuscript ID	cjfas-2016-0290.R1
Manuscript Type:	Article
Date Submitted by the Author:	23-Nov-2016
Complete List of Authors:	Goethel, Daniel; Southeast Fisheries Science Center, Berger, Aaron; NOAA-NMFS, FRAM
Keyword:	POPULATION STRUCTURE < General, SPATIAL ANALYSIS < General, FISHERY MANAGEMENT < General, STOCK ASSESSMENT < General, MOVEMENT < General

Title: Accounting for Spatial Complexities in the Calculation of Biological Reference Points: Effects of Misdiagnosing Population Structure for Stock Status Indicators

Running Title: Impact of spatial stock structure on the calculation of biological reference points

Daniel R. Goethel[a, 1] and Aaron M. Berger[b]

[a] Sustainable Fisheries Division, Southeast Fisheries Science Center, National Marine Fisheries Service, National Ocean and Atmospheric Administration, 75 Virginia Beach Drive, Miami, FL 33133, USA

[b] Fisheries Resource and Monitoring Division, Northwest Fisheries Science Center, National Marine Fisheries Service, National Oceanic and Atmospheric Administration, 2032 S.E. OSU Drive, Newport, OR 97365, USA

[1] Corresponding author (tel: +1 305.361.5761; e-mail: daniel.goethel@noaa.gov)

Abstract

Misidentifying spatial population structure may result in harvest levels that are unable to achieve management goals. We developed a spatially-explicit simulation model to determine how biological reference points (BRPs) differ among common population structures, and to investigate the performance of management quantities that were calculated assuming incorrect spatial population dynamics. Simulated reference points were compared across a range of population structures and connectivity scenarios demonstrating the influence of spatial assumptions on management benchmarks. Simulations also illustrated that applying a harvest level based on misdiagnosed spatial structure leads to biased stock status indicators, overharvesting or foregone yield. Across the scenarios examined, incorrectly specifying the connectivity dynamics (particularly misdiagnosing source-sink dynamics) was often more detrimental than ignoring spatial structure altogether. However, when the true dynamics exhibited spatial structure, incorrectly assuming panmictic structure resulted in severe depletion if harvesting concentrated on more productive population units (instead of being homogenously distributed). Incorporating spatially-generalized operating models, such as the one developed here, into management strategy evaluations (MSEs) will help develop management procedures that are more robust to spatial complexities.

Keywords: spatial population structure, biological reference points, maximum sustainable yield, overfishing, fisheries management, population dynamics, connectivity, stock assessment

Introduction

Fish movement and dispersal stem from a variety of biotic and abiotic factors (Bowler and Benton 2005) and contribute to a continuum of genetic variation and associated population structures (Reiss et al. 2009; Ciannelli et al. 2013). Spatial connectivity is an important facet of fish population dynamics that helps safeguard population units against natural and anthropogenic perturbations and maintains population stability (Kerr et al. 2010a,b). The spatial distribution of fishing effort can also influence population structure and displacement of effort has been used as a management tool for implementing conservation strategies (e.g., implementing Marine Protected Areas; Punt and Methot 2004; McGilliard et al. 2015). Protecting and conserving spatial population structure has been a central concern for rational fisheries management for over a century (Hjort 1914; Beverton and Holt 1957; Sinclair 1988; Cadrin and Secor 2009).

There has been increasing effort in recent decades to incorporate spatial heterogeneity in population and fishery dynamics into stock assessment (and ecosystem) models that underlie management advice (see review by Goethel et al. 2011), and to develop marine policies that directly protect spatial population structure, including sub-population components (e.g., spawning populations; Kritzer and Liu 2014). However, spatial structure is rarely concurrently and holistically evaluated across the entire assessment-management interface. The spatial scale of stock assessment models is often limited by the available data, which, until recently, has typically been reported by broad-scale management units (Wilen 2004). Consequently, the ability to achieve the desired objectives of fine-scale fishery regulations is severely hampered by using outputs of stock assessments that do not match the desired spatiotemporal scale (Cope and Punt 2011; Goethel et al. 2016).

Simulation experiments that evaluate spatial processes can be useful tools for understanding the importance of spatial population structure for the sustainable management of marine resources (e.g., Pelletier and Mahévas 2005; Kerr and Goethel 2014). In certain cases, it has been demonstrated that spatially-aggregating data or assessment results across known spatial components may be warranted or even statistically advantageous, particularly if there is little genetic differentiation or sample sizes are limited (Li et al. 2015; Benson et al. 2015; Goethel et al. 2015; Punt et al. 2015). However, the majority of spatial simulations have indicated that ignoring spatial structure is likely to be detrimental either to the resource, the harvesters or both (for reviews see Kerr and Goethel 2014 and Goethel et al. 2016).

When management (e.g., setting of catch quotas) ignores population structure or connectivity among population units, there is increased potential for overharvesting and system productivity is often incorrectly estimated (Fu and Fanning 2004; Kerr et al. 2014; de Moor and Butterworth 2015). Even when population structure is recognized and accounted for within the management framework, if the spatial dynamics of the fishery (e.g., gear selectivity or effort) are ignored, the possibility of overharvesting can remain (Fahrig 1993; Mchich et al. 2006; Ling and Milner-Gulland 2008; Benson et al. 2015; Hoshino et al. 2014). Concomitantly, underharvesting can also occur when effort is not efficiently allocated between spatial units, resulting in foregone yield and lower net revenue for fishing fleets (Tuck and Possingham 1994). Because harvest strategies are often context-dependent, no single, optimal approach to distributing fishing effort exists when spatial structure is present (Steneck and Wilson 2010). For instance, the optimal strategy when source-sink dynamics are modeled has been shown to differ between focusing

harvest on the source or the sink population, exclusively, depending on modeling assumptions and management objectives (Tuck and Possingham 1994; Sanchirico and Wilen 2001, 2005; Wilberg et al. 2008).

Spatial dynamics can complicate the determination of management benchmarks, because of the multi-level spatiotemporal interactions that occur among individual fishermen behavior (targeting), differences in gear selectivity among fleets, regulatory management, and the underlying population demographics (Steneck and Wilson 2010; Goethel et al. 2016; Thorson et al. 2016, this issue). Surplus production models have been used to estimate maximum sustainable yield (MSY) when metapopulation dynamics exist and sub-populations are linked through movement or recruitment dynamics (Carruthers et al. 2011; Takashina and Mougi 2015). For instance, using a metapopulation operating model, Ying et al. (2011) demonstrated that ignoring metapopulation structure led to localized depletion, because biased stock status indicators were estimated from spatially-aggregated surplus production models. Yield-per-recruit (YPR) and spawner-per-recruit (SPR) models have also been adapted to account for spatial structure within a population by allowing movement among population patches (e.g., Beverton and Holt 1957; Punt and Cui 2000) or by addressing heterogeneity in effort and population distribution using individual-based models for sessile species (Hart 2001, 2003; Truesdell et al. 2016). When stock-recruitment dynamics are accounted for directly, slightly more complex simulation models can be utilized to calculate a suite of potential spatially-explicit reference points. For example, Kerr et al. (2014) illustrated how accounting for population structure and genetic straying (i.e., connectivity among spawning components) in Gulf of Maine

115 cod could lead to different interpretations of population productivity and system yield compared
116 to spatially-aggregated models.
117
118 However, there are few instances of integrated assessment-management frameworks that
119 incorporate spatial structure into both the stock assessment model and the resulting simulations
120 of management benchmarks or yield projections. For tuna in the western and central Pacific
121 Ocean, the MULTIFAN-CL software program (Fournier et al. 1998; Hampton and Fournier et al.
122 2001) is used to provide spatially-explicit estimates of exploitation by modeling catch by region
123 and allowing connectivity among regions. In many applications, a single interbreeding
124 population is modeled allowing equilibrium yield or depletion (relative to unfished levels) based
125 reference points to be defined for the entire population (or system) without a mismatch in spatial
126 structure. However, recent modeling additions allow performing these analyses regionally,
127 thereby preserving the same connectivity and fishery dynamics utilized in the assessment model
128 (J. Hampton, SPC, Nouméa, New Caledonia, personal communication, 2016). Similarly,
129 assessment of the snapper resource in New Zealand is undertaken utilizing a spatially-explicit
130 model (i.e., a customized version of the CASAL software program; Bull et al. 2012) to
131 simultaneously model the three populations in the SNA1 management unit (Francis and
132 McKenzie 2015). This model assumes that each population exhibits natal fidelity (i.e., natal
133 homing) and connectivity is incorporated by calculating the degree of spatial overlap within each
134 geographic zone, while allowing individuals to perform instantaneous spawning migrations to
135 their natal population's spawning area. Population-specific virgin biomass (B_0) estimates are
136 utilized in conjunction with deterministic B_{MSY} simulations to determine stock status, which
137 explicitly accounts for connectivity dynamics and provides reference points both by geographic

area and by population unit. Although SNA1 snapper provides one of the few examples of a complete spatially-explicit assessment-management framework, many uncertainties exist particularly regarding population structure and connectivity assumptions (Francis and McKenzie 2015).

Despite increasing awareness that fishery and population spatial structure have important implications for defining management benchmarks and resulting harvest levels, investigations have often been focused on a single application involving only one or two assumed population structures. We develop a spatially-explicit simulation framework that can account for a variety of spatial processes, then apply it across a relatively comprehensive range of common spatial population structures and connectivity dynamics to provide a broad comparison of resulting biological reference points. Next, we demonstrate the management implications of misdiagnosing population structure by exploring the potential for overharvest and loss of yield when harvest levels are applied based on incorrect management benchmarks. By improving our understanding of the consequences associated with misidentifying population structure at the assessment-management interface (e.g., the conversion of assessment outputs into management advice), resource managers will be better able to identify potential harvest policy pitfalls and prioritize limited management resources (e.g., to determine the cost/benefit of fine-scale data collection; Goethel et al. 2016).

Methods

A generalized simulation framework was built to utilize stock assessment input (e.g., life history and demographics) and output values (e.g., terminal year abundance, natural mortality, fishery

161 selectivity, and recruitment parameter estimates) in order to project resource dynamics assuming
162 a particular spatial population structure and associated connectivity dynamics. The purpose of
163 the framework was twofold: to determine reference points under a variety of assumed spatial
164 dynamics and to address the management implications of applying a harvest level developed
165 with misdiagnosed spatial dynamics (Figure 1).
166
167 ***Generalized Simulation Model***
168 The age-structured population dynamics are described below, but for further details see Goethel
169 et al. (2011; Section 4). Each implementation of the model differs only in the assumed
170 population structure and connectivity dynamics. Table 1 provides a glossary defining important
171 terms used throughout the article.
172
173 The model was designed to perform simulations in two stages using both AD Model builder
174 (ADMB; Fournier et al. 2012) and Program R (R core team 2012) statistical computing software.
175 The first stage determined biological reference points (BRPs; Figure 1). Model inputs were used
176 to simulate population dynamics forward through time until equilibrium was reached. An
177 iterative search algorithm was implemented that ran the model across combinations of fishing
178 mortalities (according to a defined step size for each fleet and area) to find the desired BRP. In
179 the current study, SSB_{MSY} (achieved by fishing at the harvest rate, u_{MSY}, that achieved the
180 maximum system yield) was used as a BRP for comparative purposes. However, the model
181 search algorithm could be setup to achieve any number of alternative depletion or yield-based
182 BRPs.
183

The second stage determined the impact of fishing at alternative harvest levels (Figure 1). Instead of using the search algorithm to find the desired BRP, a harvest rate (or yield) was specified and the model dynamics were simulated forward using this value at the appropriate scale (i.e., system-wide or area-specific values could be input). The primary function was to investigate the impact of misdiagnosing spatial population dynamics by fishing at the harvest rate that achieved the desired BRP in stage 1, but for an incorrectly assumed spatial structure (i.e., the input harvest rate did not achieve the BRP for the true simulated population structure). The Newton-Raphson method was utilized to iteratively tune the model until the fishing mortality that corresponded to the desired harvest rate by area was approximated within a certain error threshold. The default assumption when applying harvest rates was that fishing effort was homogenously distributed across areas. When the applied harvest rate was for an assumed single area population, but the true dynamics contained multiple areas, the harvest rate was evenly applied to all areas. Other effort allocation assumptions could be applied across areas to approximate concentration of fishing effort, while still being constrained to maintain the same overall (i.e., system-wide) input harvest rate.

Population Structure

The population structure was defined by the number of population units, the interactions among units, and the recruitment dynamics. Four types of population structure were considered corresponding to the main types typically modeled in spatially-explicit stock assessments (Goethel et al. 2011): panmictic, single population with spatial heterogeneity, multiple populations with natal homing, and metapopulation structure (Figure 2A). When defining each of these population structures, careful consideration of definitions is warranted, especially in the

determination of geographic units versus population units. For the purposes of this study, an 'area' was defined as a geographic unit representing the spatial extent over which a homogenous fishing mortality acted. Depending on the type of population structure, an area may contain a segment of a single population, an entire population or segments of multiple populations. A population was defined as a self-reproducing biological entity within which all fish were able to reproductively mix resulting in a single spawning stock biomass (SSB) that determined population-specific recruitment values based on a unique stock-recruit function. Depending on the type of population structure, area and population may be synonymous or a population may be scattered across multiple areas.

Panmictic structure was defined as a single reproductively mixing population where no spatial structure existed (i.e., fish were well-mixed throughout the area). A unit population was assumed such that all fish were homogenously distributed across a single area and no immigration or emigration occurred. A single stock-recruit function was utilized with all mature fish in the population contributing to the SSB. Panmictic structure represents the simplest possible population structure and is one of the most common assumptions in stock assessment models.

When spatial structure was assumed to occur within a single population, the resulting spatial heterogeneity was modeled by allowing multiple areas within the population. A single stock-recruit function was utilized with SSB summed across all areas. A single genetic population was assumed to come from a single larval pool. Total abundance before movement, N_{BEF}, at the youngest age, a_0, for a given population (j) and year (y) was a function (based on the stock-

recruit relationship) of the total SSB summed across all areas (r), while the area-specific abundance at the youngest age was the total abundance multiplied by the apportionment factor (ξ) for that area:

$$N^{\Sigma r}_{j,y,a_0,BEF} = f\left(\sum_a SSB^{\Sigma r}_{j,y,a}\right)$$

$$N^{r}_{j,y,a_0,BEF} = \xi^r_j N^{\Sigma r}_{j,y,a_0,BEF}$$

(1)

A wide variety of species exhibit some degree of spatial heterogeneity in distribution, despite maintaining a single reproductive population (e.g., Gulf of Alaska sablefish; Hanselman et al. 2015).

Metapopulation structure was defined similarly to a single population with multiple areas, except that multiple populations were modeled simultaneously. Reproductive mixing occurred among populations, through the movement of mature individuals, but each population was assumed to maintain its own larval pool. For metapopulation dynamics, area and population delineations were now synonymous (i.e., $r = j$), because once a fish moved into another area it assumed the reproductive dynamics and demographics of the population residing in that area. Basically, a fish was instantaneously exposed to the dynamics of the population that inhabited the area that it currently occupied, which assumed that environment was the main driver of life history (not genetics). The recruitment dynamics followed Equation 1, but multiple populations were modeled simultaneously each of which maintained its own stock-recruit function defined by the SSB of all fish currently residing in the corresponding area. Metapopulation structure is becoming a more widely observed form of population structure for marine fish, and is frequently

250 detected in reef fish and small pelagics (e.g., Atlantic herring; Kritzer and Sale 2004; Kerr et al.
251 2010b)
252
253 Natal homing (also known as the overlap model; Porch 2003) was the most complex population
254 structure evaluated. Multiple populations were modeled, but no reproductive mixing occurred
255 among them. Similar to a metapopulation, each population unit maintained its own stock-recruit
256 relationship. However, fish only contributed to the SSB of their natal population. As individuals
257 moved among population areas, they cohabitated with fish of other natal populations but were
258 unable to reproduce with them. Because of the overlap of non-interbreeding populations within
259 an area, area was no longer equivalent to population (i.e., $r \neq j$). Once again, recruitment was
260 based on Equation 1. Contrary to metapopulation structure where recruitment was determined
261 from all the SSB in the given population area, natal homing implied that individuals not within
262 the confines of their natal population area could not reproduce unless they underwent a spawning
263 migration (see Equation 2 in the following section for a description of SSB calculations for
264 alternative natal homing scenarios). Demographics were now assumed to be defined by the natal
265 population (i.e., vital rates no longer changed as an individual moved among areas), which
266 implied that life history characteristics were determined by genetics (not environment). Natal
267 homing has been hypothesized for many large pelagics (e.g., Atlantic bluefin tuna; Rooker et al.
268 2008) and is a well-known trait for salmon.
269
270 *Movement Parametrization*
271 Simulated movement used the box-transfer method, which assumed a certain fraction of the
272 population instantaneously moved to the other areas at the beginning of the year. The movement

parameter, $T_{j,y,a}^{r\to s}$, represented the fraction of fish from population *j* in year *y* at age *a* that moved from area *r* to area *s* (for the simulation scenarios presented here movement was time-invariant). The population subscript changed to the new population area superscript (i.e., movement was a Markovian process) for metapopulation structure, but not for natal homing (i.e., movement characteristics were defined by the natal population). Age-specific movement was incorporated by allowing different movement rates for the youngest age class compared to all other age classes. The primary assumption was that if, for example, the model started at age-0 (i.e., the stock-recruit function provided the number of age-0 eggs or larvae), then age-0 movement would represent larval drift and would be characterized by different dynamics than the movement of older fish. Additionally, it was assumed that apportionment of larvae and larval drift were separate processes (i.e., age-0 larvae were apportioned to area, and then allowed to move among areas).

Two unique movement scenarios were examined using the natal homing population structure. Spawning migrations were incorporated by defining a probability of returning, *Pr(SpawnReturn)*, as the fraction of the natal population not in the natal area that returned to spawn, and which was assumed to occur instantaneously at the time of spawning. In this case, a fish could add to the SSB of its natal population, despite residing in a non-natal area (i.e., as a result of the instantaneous spawning migration):

$$N_{j,y,a_0,BEF}^{r=j} = f\left[\sum_a SSB_{j,y,a}^{r=j} + \sum_{r,r\neq j}\left(\Pr(SpawnReturn)_j^r * \sum_a SSB_{j,y,a}^{r\neq j}\right)\right]$$

$$N_{j,y,a_0,BEF}^{r\neq j} = 0 \qquad \textbf{(2)}$$

By accounting for fish that did not contribute to SSB, the spawning migration probability effectively allowed for skipped spawning (i.e., mass resorption of oocytes), which has been observed in some species that demonstrate natal homing (e.g., Atlantic cod and bluefin tuna; Rideout and Tomkiewicz 2011).

The second movement scenario (termed natal return; Table 1) was defined to approximate ontogenetic movement. Movement was allowed at the initial age (i.e., larval drift). A permanent return migration to the natal area could then occur at a certain age, a_{RET}, with a probability given by *Pr(PermReturn)*. Movement was not allowed at any other ages. Recruitment was thus a function of the SSB in the natal population area plus the corresponding SSB of fish that moved back to the natal population at a_{RET}:

$$N_{j,y,a_0,BEF}^{r=j} = f\left[\sum_{a} SSB_{j,y,a}^{r=j} + \sum_{r,r\neq j} \left(\Pr(PermReturn)_j^r * SSB_{j,y,a=a_{RET}}^{r\neq j}\right)\right] \quad \textbf{(3)}$$

With this scenario, fish that did not return (according to a_{RET}) never contributed to the SSB. This configuration was meant to approximate an ontogenetic migration back to the natal population once a fish had reached maturity. The basic ecological premise was that larval or young-of-the-year fish settled and spent their juvenile stage in various areas (e.g., nursery grounds) where they did not contribute to the SSB. Then, once maturity was reached, adult fish would move back to the natal population and contribute to SSB (assuming negligible straying). Ontogenetic migrations have been observed in a number of species (e.g., Gulf of Alaska sablefish; Hanselman et al., 2015), and has been hypothesized in conjunction with natal homing for some large pelagics (e.g., Atlantic bluefin tuna; Rooker et al. 2008). Although the implemented natal return

scenario does not explicitly match any known ontogenetic migration patterns, it represents a first approximation to the more complex versions seen in the real world.

Population Dynamics

Abundance was projected forward from input initial abundance-at-age and calculated recruitment at the minimum age (Figure 2B). Recruitment calculations assumed a Beverton-Holt stock-recruit model, where SSB was calculated based on weight and was adjusted based on the assumed population structure and movement dynamics (as described above) and for the time of spawning. Mortality was assumed to be a function of area. Fishing mortality was separated into an area- and fleet-specific yearly multiplier, F, and an age-specific selectivity component. Selectivity, v, for each of the modeled fleets, f, was input directly by age. Any number of fleets was allowed within each area (for the simulation scenarios presented here only one fleet per area was modeled). Natural mortality, M, was input directly and could vary by age, year, and area. In the recruitment year, mortality was discounted for the fraction of the year that fish underwent mortality based on the time of spawning (and hence birthdate). Abundance-at-age at the beginning of the year before movement, N_{BEF}, in area r from natal population j in year y and at age a was calculated from the abundance after movement, N_{AFT}, in the previous year and age as:

$$N^{r}_{j,y,a,BEF} = N^{r}_{j,y-1,a-1,AFT} e^{\left[-\left(F^{r,\Sigma f}_{j,y-1,a-1} + M^{r}_{j,y-1,a-1}\right)\right]}$$

$$F^{r,\Sigma f}_{j,y-1,a-1} = \sum_{f} v^{r,f}_{j,y-1,a-1} F^{r,f}_{j,y-1}$$

(4)

The terminal age was assumed to be a plus group that was the summation of all fish that survived to the plus group age from the previous age along with all fish already in the plus group that

survived to the next year. Instantaneous movement immediately followed at the start of the year, and abundance-at-age after movement, N_{AFT}, was:

$$N^{r}_{j,y,a,AFT} = \sum_{s} T^{s \to r}_{j,y,a} N^{s}_{j,y,a,BEF} \quad \textbf{(5)}$$

Catch-at-age, C_a, was calculated using Baranov's catch equation based on the area- and fleet-specific mortality and selectivity values and the available abundance after movement, while yield, Y, was the summation over age of catch-at-age multiplied by the weight-at-age, w:

$$C^{r,f}_{j,y,a} = N^{r}_{j,y,a,AFT}\left(1 - e^{\left[-\left(F^{r,\Sigma f}_{j,y,a} + M^{r}_{j,y,a}\right)\right]}\right)\frac{v^{r,f}_{j,y,a} F^{r,f}_{j,y}}{F^{r,\Sigma f}_{j,y,a} + M^{r}_{j,y,a}}$$

$$Y^{s,r,f}_{j,y} = \sum_{a}\left(C^{r,f}_{j,y,a} * w_{j,y,a}\right) \quad \textbf{(6)}$$

The general spatial and spatiotemporal dynamics are illustrated in Figures 2A and 2B.

Model Outputs

Several output quantities that are typically important for making management decisions were provided for each year of the simulation and at all spatial scales (i.e., system-wide or by area). By providing results at different spatial scales, the impacts of applying a given mortality rate could be examined at different levels, which can be particularly useful when comparing different types of assumed population structures. Results were also provided by area and by natal population in order to allow comparison among different population structures. Biological metrics included: abundance-at-age, recruitment, biomass, SSB, depletion ($biomass_{Current}/biomass_{Initial}$), and spawning potential ratio (SPR = $SSB_{Current}/SSB_{0,}$ where SSB_0

was calculated based on unfished equilibrium SSB and the parameters of the stock-recruit curve). Mortality-based metrics included: catch-at-age, yield, and harvest rate or exploitation fraction (yield/biomass).

Model Application

The generalized framework was applied to evaluate three main study objectives using MSY-based reference points. MSY-based reference points were chosen for illustrative purposes, because they are widely used (as explicit or proxy reference points) and discussed in fisheries management. However, their use is not meant to represent the basis for any particular real-world harvest policy. For the first objective (*BRP_Dev*), the stage 1 model (Figure 1) was run for several alternative spatial population structures and various connectivity dynamics, and the resulting MSY-based reference points were compared. The second objective (*HL_App*) applied results from the stage 1 model runs to the stage 2 model (Figure 1), where an MSY-based harvest level was applied based on an incorrect assumption regarding spatial structure and connectivity dynamics. Thus, the dynamics of the true population structure were simulated using the harvest rate that achieved MSY for the assumed population structure. Model outputs (e.g., level of depletion, foregone yield, and bias in stock status indicators) were then compared across scenarios. The simulation model for objectives one (*BRP_Dev*) and two (*HL_App*) was conditioned to loosely emulate a mid-water pelagic, hake-like species with many of the life history characteristics borrowed from the Pacific hake (*Merluccius productus*) stock assessment (Grandin et al. 2016). This species was chosen to provide realistic parameters to initialize the model (see Table 2 for input values), but, given the many simplifying assumptions made, the results were not meant to be representative for any particular species and thus were not suitable

as the basis for management advice. The third objective (*Snapper_App*) was to apply the generalized simulation framework (stages 1 and 2) to a species with alternative life history parameters and to explore the impact of spatial effort allocation. The input parameters, spatial population structure, and connectivity scenarios were based on aspects of Gulf of Mexico red snapper (*Lutjanus campechanus*), though model evaluations are exploratory and not suitable as the basis for management advice.

Base Dynamics and Scenarios: Mid-water Pelagic

The simulation model used to evaluate objectives one (*BRP_Dev*) and two (*HL_App*) was first parameterized by a base set of population dynamics and then adjusted to evaluate alternative spatial structure and connectivity scenarios. The base model assumed 15 ages and deterministic simulations were carried out for 200 years, a time period meant to allow equilibrium conditions to occur. The initial age-structure was setup so that abundance at the youngest age class was equivalent to R_0 (virgin recruitment; 3.125 million fish), and the abundance-at-age was at unfished equilibrium assuming an age-invariant natural mortality of 0.226, but adjusted such that the total SSB was equivalent to SSB_0 (virgin spawning stock biomass; 2.397 million mt). A Beverton-Holt stock-recruit function was assumed with a steepness of 0.814, and no stock-recruit deviations were incorporated. SSB was in weight and weight-at-age was input in kilograms. A single fleet was assumed for each area and selectivity was set equivalent to maturity in order to avoid any influence of differences in these quantities on results. All parameters were time-invariant (see Table 2 for input parameter values).

For population structures assuming multiple areas, the number of areas was two for tractability and ease of interpretation of results. The vital rates were assumed constant across all areas or populations and R_0, SSB_0, and initial abundance-at-age were evenly apportioned among populations in order to ensure that results were not influenced by differential population demographics and that differences in spatial dynamics were the axis of evaluation. For scenarios where differential recruitment apportionment or productivity among areas was assumed, the first area had the potential to produce up to 30% of the total recruitment, while the second area could produce up to 70%. For a single population with multiple areas, this was accomplished by splitting the recruitment apportionment factor 30/70 (instead of the base 50/50 split). For multiple population scenarios, the split was achieved by scaling the population-specific R_0 and associated SSB_0, which then also required rescaling the initial abundances-at-age.

Movement rates and types differed according to objective and scenario set. Movement was separated between larval drift (constant movement at age a_0) and adult movement (constant movement for ages greater than a_0). Two levels of movement were evaluated (high or low residency) along with two types of movement (bidirectional or unidirectional), and both could occur at the larval or adult stage. Bidirectional movement allowed fish to move between both areas, while unidirectional movement represented source-sink dynamics (i.e., fish move in one direction). For bidirectional movement, high residency indicated that 80% of fish stayed in area 1 and 85% stayed in area 2 in any given year, while low residency indicated that 60% stayed in area 1 and 65% stayed in area 2. For unidirectional movement, fish were only allowed to move from area 2 to area 1 (representing movement from the more productive area to the less productive area when productivity differed) with high residency set to 85% and low residency to

65%. For natal homing scenarios, spawning migrations and natal return were considered. The probability of return was 75% for spawning migrations and constant across population areas, which represented a plausible level given recent literature on skipped spawning (Rideout and Tomkiewicz 2011). For the natal return models, high and low return probabilities (85% or 65%, respectively) were evaluated, where the age of return was set to age-4 (roughly corresponding to 75% maturity). Alternative movement levels were chosen to provide a reasonable range of plausible rates but, again, were not meant to reflect any particular species.

Scenarios for the first objective (*BRP_Dev*) were developed to calculate and compare reference points across different spatial structures and connectivity assumptions. The first subset of scenarios focused on the role of adult movement (*Adult_Move*; a complete listing is provided in Supplementary Material Table S1). The second subset looked at the impact of larval connectivity (*Larval_Move*; Supplementary Material Table S2). The third subset allowed both adult and larval connectivity (*All_Move*; Supplementary Material Table S3). The fourth subset demonstrated the impact of full connectivity dynamics along with variation in recruitment (i.e., productivity) across areas (*Move+Prod*; Table 3).

Scenarios for the second objective *(HL_App*) were developed using model output harvest levels from the high adult and high larval residency scenarios of objective one, subset four (*Move+Prod*), as these represented the most inclusive set of MSY-based harvest levels examined. For each scenario, there was a true underlying spatial structure that determined the dynamics of the system and an assumed spatial structure that was used to guide management (i.e., the implemented harvest level) for the true system. The applied harvest rate was that which

443 maximized yield (u_{MSY}) for the assumed spatial structure. For situations where the assumed
444 spatial structure was panmictic, the panmictic u_{MSY} was applied to each of the areas in the true
445 population structure. On the other hand, when multiple areas were assumed but the true structure
446 was panmictic, the system-wide u_{MSY} from the assumed structure (i.e., the total u_{MSY} across all
447 areas) was used as the harvest rate for the panmictic population. When multiple area spatial
448 structures were examined for both the assumed and true dynamics, the assumed u_{MSY} for the first
449 [second] area was applied to the first [second] area in the true dynamics. Resulting area-specific
450 and system-wide terminal year outputs (e.g., SSB, yield, and SPR) allowed comparison of how
451 misdiagnosing spatial structure and unknowingly implementing inappropriate management
452 harvest levels may affect the ability to achieve long-term management goals.
453
454 *Base Dynamics and Scenarios: Red Snapper-like*
455 The simulation model used to evaluate objective three (*Snapper_App*) was also parameterized by
456 a base set of population dynamics (Supplemental Table S4), but some simplifying assumptions
457 were made compared to the current assessment (e.g., only a single fleet per area was modeled
458 here). Reference points were evaluated based on various hypothesized spatial structure and
459 connectivity scenarios. For red snapper, spatial structure is known to exist, but the causes and
460 levels of potential mixing among areas is not well known (Patterson 2007; Karnauskas et al.
461 2013). The current stock structure applied to the assessment of red snapper is essentially two
462 populations (eastern and western Gulf of Mexico) with management treating them as a single
463 population, but tagging studies and larval drift models indicate that metapopulation structure
464 may exist (Patterson 2007; Karnauskas et al. 2013).
465

466 Life history parameters were derived from the most recent stock assessment (SEDAR 2015), but
467 some parameters were altered to fit the various modeling assumptions. All parameters were
468 assumed constant across areas (as was done in the stock assessment) and were time-invariant.
469 Selectivity was taken from the dominant fishery (the recreational fleet in the eastern area) in
470 order to avoid the added complexity of averaging selectivity across fleets when a single
471 panmictic population was assumed. The assessment fixes steepness at 1.0, but allows a time-
472 varying recruitment distribution parameter in order to accommodate the independent recruitment
473 that is thought to exist between the eastern and western populations. For this study, steepness
474 was fixed at 0.85 in order to maintain the reliance of recruitment on SSB. When evaluating a
475 single population with two areas, the recruits were apportioned using the time-averaged
476 apportionment factor estimated from the stock assessment (66% of recruits are apportioned to the
477 western area, referred to as area 2 here). When evaluating metapopulation models, R_0 was
478 apportioned using the same ratio.
479
480 Three types of population structure were investigated based on previously hypothesized
481 connectivity dynamics (Patterson 2007): panmictic, a single population with two areas, and
482 metapopulation structure. For the two spatial population structures, different connectivity
483 dynamics were investigated based on larval connectivity hypothesized from a larval individual-
484 based model (IBM) developed for red snapper (Karnauskas et al. 2013). Five movement
485 scenarios were considered: no movement; bidirectional larval movement with average values
486 from the larval IBM (~97% residency for each population); unidirectional larval movement at
487 maximum values from the larval IBM (the eastern, area 1, or western, area 2, is treated as a
488 source with residency of 93%); unidirectional larval movement based on hypothesized maximum

values (the eastern, area 1, or western, area 2, is treated as a source with residency of 80%); and bidirectional average larval movement (97% residency) with bidirectional adult movement based on hypothesized movement rates (90% adult residency for each population).

Associated reference points were developed for each population structure (see Table S5 for a list of scenarios), and then MSY-based harvest levels were applied to investigate the impact of misdiagnosing spatial structure when effort was apportioned evenly among areas (*Snapper_Even_Eff*; see supplemental Figure S14 for specific scenarios). Uneven apportionment of effort was also evaluated when panmictic stock structure was assumed (*Snapper_Uneven_Eff*; see Figure 7 for specific scenarios), such that the input harvest rate on the eastern population (area 1) was halved and the harvest rate on the western population (area 2) was increased until the panmictic u_{MSY} was achieved for the entire complex. The *Snapper_Uneven_Eff* scenarios illustrated the detriments of ignoring population structure when management failed to limit harvesting aggregation, and were meant to touch upon the potential impact that spatial fleet dynamics (and lack of sub-population catch allocations) might have on naïve management strategies.

Graphical Analysis

For all scenarios, model output comparisons were carried out through graphical analysis of important management quantities (e.g., MSY, SSB_{MSY}, and u_{MSY}). When evaluating the impact of misdiagnosing spatial population structure, results were presented as the ratio of the terminal yield or SSB compared to either the true MSY or SSB_{MSY} or the assumed MSY or SSB_{MSY}. Yield comparisons provided an indication foregone yield, while SSB comparisons indicated the

level of depletion and bias in a common stock status indicator (i.e., when compared to the true stock status).

Results

Development of BRPs (BRP_Dev)

Spatial population structure had important implications for resulting spatially-explicit management harvest levels and biological reference points (*Move+Prod* scenario results are described here and qualitatively summarized in Table 4; *Adult_Move*, *Larval_Move*, and *All_Move* scenario results are shown in Supplemental Figures S1, S2, and S3, respectively). Although system-wide (total) u_{MSY} was relatively constant across population structures and connectivity dynamics (with the exception of a few cases), resulting SSB_{MSY} varied considerably across scenarios (Table 4, Figure 3). In addition, different area-specific harvest rates were required to maximize utilization across population structures (Figure 3). For instance, when source-sink dynamics were present, the source population remained relatively unfished (u_{MSY} was less than 0.05), whereas the sink population was fished much harder (u_{MSY} was near 0.4). These results held for both metapopulation and single population, two area scenarios, but were less pronounced (area-specific u_{MSY} ranged from 0.15 to 0.23) for the natal homing scenarios (Figure 3). The resulting system-wide SSB_{MSY} was the lowest for the source-sink metapopulation dynamics, due to the constant loss of SSB (and consequent recruitment) from the source population. Adult connectivity was a more important factor than larval connectivity in driving the lower SSB_{MSY} for source-sink dynamics (scenarios 13 and 15 versus 12 and 14 in Figure 3), because losses due to movement occurred at every adult age instead of just the youngest age of the cohort (i.e., when only larval connectivity was considered).

Similarly, differential recruitment exacerbated the relative differences in management quantities across areas. Because fish always added to the SSB of their current resident area for the non-natal homing scenarios, it was intuitive that the area receiving a subsidy (i.e., the sink) would be able to sustain a higher fishing pressure. Interestingly, the results for bidirectional movement began to mimic source-sink dynamics when productivity differed among populations (e.g., scenarios 17 and 19, Figure 3). When there was a metapopulation with bidirectional movement and differential productivity, the more productive population needed to be protected, while harvest on the less productive population could be much higher. However, with bidirectional movement the loss of individuals to the less productive population could be offset by immigration from the *de facto* sink population (i.e., SSB_{MSY} was higher than for the true source-sink scenarios).

For natal homing scenarios, system-wide SSB tended to be lower, but fluctuations in area-specific harvesting rates (range of 0.15-0.25) were not as strong as for metapopulation structure (range of 0.05-0.45; Figure 3). When no spawning migrations were assumed to occur with unidirectional movement, system-wide SSB_{MSY} and associated u_{MSY} declined by about 15% resulting in a 5% decline in MSY compared to the same scenarios with spawning migrations. These results were more pronounced for bidirectional movement (declines around 25% for SSB_{MSY} and u_{MSY} with a 10% reduction in MSY). Because fewer fish moved under source-sink dynamics than with bidirectional movement, it was not surprising that SSB_{MSY} was lower for the latter because more fish resided outside their natal area and contributed less to natal SSB.

558 *Application of Incorrect Harvest Levels (HL_App)*

559 The risk of depleting certain areas (within or among populations) while underutilizing others
560 differed across the scenarios examined, but tended to be greatest when the true population
561 structure involved metapopulation dynamics (results are qualitatively summarized in Table 5).
562 Ignoring spatial population structure (i.e., assuming panmictic structure) was not as detrimental
563 as might otherwise be expected for system-wide status (in terms of terminal SSB compared to
564 the true SSB_{MSY}), but it could lead to significant depletion of individual areas (Figure 4; Table
565 5). When the underlying dynamics involved source-sink connectivity, assuming no spatial
566 structure led to the source area being severely overharvested (SSB less than 40% of SSB_{MSY} for
567 metapopulation structure) with the sink area being underharvested (SSB over 150% of SSB_{MSY}
568 for metapopulation structure). Moreover, for metapopulation structure with source-sink
569 dynamics a 25% loss of yield resulted due to misdiagnosing stock structure (Supplemental
570 Figure S5). The main problem with assuming no structure was that managers would only be
571 provided stock status on a system-wide basis, which could indicate that the system was doing
572 well regardless of area-specific depletion (Figure 4 and Supplemental Figure S4).
573
574 Interestingly, assuming metapopulation structure when it was not occurring or simply
575 misdiagnosing the connectivity dynamics when metapopulation dynamics were correctly
576 assumed, resulted in the most frequent occurrence of depleting an area (Figure 5; Table 5).
577 When metapopulation structure with source-sink dynamics were assumed, the first area was
578 consistently depleted to low levels (SSB ranged from 15 to 50% of SSB_{MSY}), while the second
579 area was underfished (SSB was 120-140% of SSB_{MSY}) regardless of the true spatial structure.
580 The system-wide SSB tended to be maintained around the true SSB_{MSY}, a notable exception

being for a single population with two areas and unidirectional movement (terminal SSB was at 60% of SSB_{MSY}). The biggest detriment occurred for area 1 (i.e., SSB around 15% of SSB_{MSY}) when the true spatial structure involved natal homing. When metapopulation structure with bidirectional movement was assumed, the implications were not as severe (minimum area-specific SSB around 50% of SSB_{MSY}). In certain situations when metapopulation structure was assumed, especially when the true spatial structure involved natal homing, there was considerable foregone yield (5-25%; Supplemental Figure S10).

The risk associated with assuming natal homing when in fact it was not occurring was relatively low in most cases. Overharvesting an area by more than 10% occurred in only four scenarios (Figure 6, Table 5), while there was mostly little foregone yield (Supplemental Figure S12). The largest impacts were seen when the true underlying structure involved source-sink dynamics (SSB in area 2 was around 30-70% of SSB_{MSY} for metapopulation or single population, two area true structure), though this result was pronounced for all true metapopulation structures examined regardless of assumed natal homing movement dynamics. Misdiagnosing connectivity dynamics when natal homing was correctly assumed had limited negative impact.

Red Snapper-like Application (Snapper_App)

Given the relatively limited level of larval and adult movement examined (Table S5), it was not surprising that the system-wide reference points only differed slightly (Supplemental Figure S13). Misdiagnosing spatial structure had limited impact on the resource (area-specific terminal SSB was within 85% of true SSB_{MSY} for all scenarios tested; Supplemental Figure S14) when effort was evenly allocated (*Snapper_Even_Eff* scenarios). However, when panmictic structure

604 was assumed and harvest effort was allowed to aggregate on the more productive area
605 (*Snapper_Uneven_Eff* scenarios), the potential for overharvesting increased drastically (system-
606 wide SSB was 75-90% of SSB_{MSY} for all scenarios tested; Figure 7). The western area (area 2)
607 was often depleted with the terminal SSB usually dropping to less than 50% of SSB_{MSY} and a
608 minimum value around 15%. However, the eastern area (area 1) was consistently well above its
609 SSB_{MSY} (ranging from 125-200% of SSB_{MSY}). For most of the true population structures
610 examined, there was around a 25% loss in yield from the system when spatial structure was
611 disregarded and effort was not homogenously distributed (Supplemental Figure S15).
612

613 **Discussion**

614 Over the last three decades, there has been increasing awareness that spatial population structure
615 is an important facet of resilience for marine species (e.g., Sinclair 1988; Pelletier and Mahévas
616 2005; Kerr et al. 2010a,b; Ciannelli et al. 2013). However, little research has been devoted to
617 describing how ignorance of spatial dynamics may impact biological reference points or the
618 reliability of management strategies (e.g., Ying et al. 2011; Hoshino et al. 2014). Our results
619 demonstrate that management benchmarks and the harvest levels required to attain them are
620 strongly influenced by the underlying population structure and connectivity dynamics. For
621 instance, with metapopulation structure, system-wide harvest rates could be maintained at higher
622 levels compared to other population structures, particularly when source-sink dynamics were
623 present, because movement did not hinder reproduction and area-specific fishing mortality
624 occurred only on a single population at any given time. Yet, it is important to carefully monitor
625 area-specific harvest rates in order to avoid overharvesting more productive units, which
626 generally act to maintain resource abundance. Alternatively, for natal homing, harvesting within

a given area occurs on multiple populations with different productivities so obtaining MSY-based BRPs necessitated moderate harvest rates in all areas. Unlike with metapopulation structure, area-specific harvest rates were generally independent of movement types and were relatively constant across areas for natal homing scenarios.

Previous studies have suggested that ignoring spatial structure can lead to overharvesting and localized depletion of sub-population components (e.g., Fu and Fanning 2004; Ying et al. 2011; Hoshino et al. 2014). Our findings further support the general concept that ignoring spatial structure and connectivity dynamics can lead to unintended consequences, and expands upon the types of spatial scenarios for which that applies. For the set of spatial scenarios examined for this study, systems that demonstrate source-sink dynamics have the highest potential to introduce problematic management performance when spatial connectivity is not accurately understood. Localized depletion was common when source-sink dynamics were misdiagnosed even though the underlying population structure may be correct. Incorrect assumptions regarding connectivity or mixing dynamics (even when spatial structure is properly defined) can lead to similar, and sometimes worse, outcomes compared to incorrectly assuming no spatial structure exists. This is problematic for stock assessment and resource management because connectivity dynamics are rarely well understood (e.g., Porch et al. 1998; Goethel et al. 2015), yet there is no good solution for dealing with this source of uncertainty in spatial population dynamics. Further research on the integration of multiple models (e.g., ensemble modeling utilizing a variety of plausible spatial hypotheses) into the stock assessment-management interface along with explorations with spatially explicit management strategy evaluations should help improve

649 understanding of the robustness of various management procedures to these and other
650 uncertainties.
651
652 It was somewhat surprising that when ignoring population structure (i.e., assuming a panmictic
653 population), a metapopulation with source-sink dynamics was the only true spatial structure
654 scenario that resulted in significant system-wide bias (>20%) in terms of stock status and yield.
655 One important factor related to this finding was that assumed and true connectivity dynamics
656 only included high residency, low movement simulations for the *HL_APP* scenarios. A
657 comparative analysis using low residency, high movement scenarios demonstrated more
658 pronounced impacts. The low movement scenarios were thought to provide a broader
659 representation of typical connectivity dynamics, but clearly the spectrum of results further
660 illustrates the importance of movement and population structure assumptions on the choice of
661 harvest strategies for marine resources.
662
663 A number of generalities and caveats exist with this work, and, to better understand the role of
664 these, further consideration and research is warranted. There were many area-specific factors
665 and assumptions (both within a single population and among populations) that could influence
666 results (e.g., degree of movement by age, size, area, and life stage, areal productivity, maturity,
667 growth, fishing effort allocation, and fleet selectivity). To keep the analysis tractable, many of
668 these factors, and the interactions among them, could not be explicitly investigated. The
669 assumed population and connectivity dynamics in the simulations conducted were reasonable,
670 yet simplified compared to real world applications. Additionally, as with most reference point
671 models, time-invariant model parameters were assumed during the deterministic projection

period. Given the flexibility of the modeling approach, it is relatively straightforward to evaluate alternative scenarios, allow for stochasticity in the projection period, and incorporate time-varying parameters and seasonal time increments. Similarly, more complex connectivity dynamics could be included (e.g., density-dependence and other functional forms). Further research is needed that closely examines the interplay between specific connectivity assumptions and the copious spatiotemporal biological, fleet, and management processes. By further developing the general framework for new and alternate assumptions regarding spatial, recruitment, and fishery dynamics, we expect that the basic understanding of how spatial processes impact fisheries management will be continually refined.

There are many unresolved issues that remain with marine spatial assessment models that could impact the reliability of simulation results. For instance, there is no best approach for dealing with the issue of demographic changes of individuals as they move between areas (R. Methot, NOAA NMFS, Silver Spring, MD, personal communication, 2016), which may only be tractable with individual-based modeling approaches. A critical defining characteristic that separates natal homing from metapopulation structure is the degree to which environment and genetics are expected to determine a population's demographic rates and the rate at which an individual will adapt to new environmental regimes. The basic theory of marine metapopulation dynamics (Kritzer and Sale 2004) implies that a fish adheres to the demographics of the area that it moves into (i.e., vital rates are essentially determined by the environment). Alternatively, natal homing dynamics imply that a fish maintains its life history characteristics regardless of where it resides (i.e., natal, via genetics or imprinting, demographics are upheld). In reality, both genetics and environment influence demographic and vital rates to some degree and both modeling

695 approaches have important limitations. When life history parameters differ by area, assuming
696 that a fish instantaneously adopts the demographics of a new area may result in a reduction in the
697 average size, weight or maturity of a fish as it moves throughout the spatial domain (i.e., rates
698 could be lower at older ages for different populations). Of course, assuming demographics are
699 purely genetic (as with natal homing) is also incomplete. Stock assessment software exists that
700 attempts to deal with these limitations by assigning vital rates to 'growth morphs' or 'platoons'
701 of fish that are assumed to have the same demographics (e.g., recruitment year-classes; Methot
702 and Wetzel 2013), but no fully satisfactory solution currently exists for spatial models.
703
704 Further, the instantaneous movement assumption continues to be an over-simplification in spatial
705 population models, because fish movement occurs across a continuum of physical, biological,
706 and chemical gradients (Turchin 1998). Miller and Andersen (2008) suggest that estimating
707 continuous time movement parameters (analogous to continuous fishing and natural mortality
708 rates) may be more appropriate for fisheries models. It might be worthwhile to test within the
709 current framework in order to illustrate the differences that result when fish are able to
710 continuously move from one mortality regime to another. However, until the causal mechanisms
711 that lead to continuous movement are better understood, it may be difficult to apply reference
712 points utilizing this assumption.
713
714 Developing more complex evaluations that include multi-component spatial dynamics like the
715 addition of differential selectivity, multiple fleets, and effort aggregation in areas of high
716 biomass concentration are appropriate next steps. The red snapper-like application with uneven
717 fishing effort demonstrated that as more complex, multi-component dynamics are included, the

718 potential pitfalls of ignoring spatial structure could be magnified. Spatial heterogeneity exists in
719 both the distribution of fishery resources and fishing effort (Fahrig 1993; Guan et al. 2013), and
720 these are often not proportional to each other across space. Accounting for only the biological
721 aspects of spatial structure does not provide a complete overview of how spatial heterogeneity
722 can impact estimation of biological reference points and related harvest strategies. The snapper-
723 like results provide an indication of the increased complexities that result from spatial effort
724 dynamics, which supports the findings of Hoshino et al. (2014). A wide body of literature on
725 Marine Protected Areas (MPAs) has demonstrated the importance of spatial harvest
726 displacement for the determination of stock status indicators and achievement of conservation
727 goals (e.g., Punt and Methot 2004; Pincin and Wilberg 2012; McGilliard et al. 2015). Further
728 work is needed to identify and understand the combined impact of both biological connectivity
729 and spatial fleet dynamics (Fahrig 1993; McGilliard et al. 2015)
730
731 Our analysis represents a first step towards better understanding the role that population structure
732 has in defining management benchmarks and subsequent harvest levels. Despite the use of
733 simplifying assumptions, the modeling approach highlighted important patterns and
734 opportunities for investigation (i.e., types of spatial dynamics) that warrant further exploration.
735 Next steps include broadening the generalized simulation model to include increased complexity
736 in the spatiotemporal, population, and fishery dynamics and to more fully account for system
737 uncertainties. An evaluation of data requirements and the associated parameter bias/variance
738 tradeoff that must be confronted when moving to multi-dimensional spatial models, where
739 sample size can become limiting, would also be beneficial. Although the results of this work
740 provide a basic understanding of the interplay between complex spatial dynamics and estimates

741 of management benchmarks for marine resources, we acknowledge that it only represents a first
742 step towards fully integrating spatial biological and fishery dynamics into fisheries policy. There
743 is a clear need for fisheries scientists and managers to be aware of spatial population structure,
744 because it can have strong implications for how to best manage a fishery to meet management
745 objectives (Fahrig 1993; Benson et al. 2015; Hoshino et al. 2014). In addition, spatial
746 heterogeneity due to fleet dynamics and regulatory measures (e.g., MPAs) only increases the
747 importance of accounting for spatial processes across the assessment-management interface
748 (Guan et al. 2013; McGilliard et al. 2015).
749
750 With the increasing recognition of the extensive interactions among time-varying spatial,
751 environmental, population, and fishery processes (Ciannelli et al. 2013), the reliance on static,
752 equilibrium models such as those traditionally used to calculate many biological reference points
753 should be reduced (Hilborn 2002; Hoshino et al. 2014). Developing management strategy
754 evaluations where the operating model is generalized to include many hypothesized spatial and
755 environmental complexities (similar to the model developed here) will allow testing the
756 robustness of management procedures to a variety of interacting dynamics, and will help
757 managers move away from harvest control rules based on BRPs developed with incomplete
758 assumptions (Butterworth and Punt 1999; Geromont and Butterworth 2015). Of particular
759 interest has been the exploration of empirically driven, spatially-explicit reference points that
760 could be used in lieu of or in tandem with conventional BRPs (Reuchlin-Hugenholtz et al. 2015,
761 2016). No matter how BRPs or harvest strategies are developed, it remains paramount that data
762 collection programs which elucidate migration pathways, connectivity dynamics, and
763 spatiotemporal population structure (e.g., genetic analyses, tagging data, larval transport, and

764 fine-scale life history data) continue to be funded and expanded in order to support development
765 of more realistic spatial models that can help guide sustainable fisheries management.
766
767 **Acknowledgements**
768 Earlier versions of this manuscript were improved with reviews from Meaghan Bryan, Mandy
769 Karnauskas, Shannon Cass-Calay, Clay Porch, Owen Hamel, James Thorson, and 3 anonymous
770 reviewers. We would like to thank the organizers, Rick Methot and Mark Maunder, of the 7th
771 World Fisheries Congress (Busan, South Korea) theme session on "Advancements in Stock
772 Assessment and Provision of Management Advice" for allowing us to present these findings
773 along with all participants whose discussion on the topic helped improve our study. We also
774 thank Dana Hanselman, Amy Schueller, Brian Langseth, Jon Deroba, Pat Lynch, Terry Quinn,
775 and Steve Cadrin for helping to stimulate the ideas that led to this manuscript. Finally, we thank
776 the National Marine Fisheries Service Office of Science and Technology branch of NOAA for
777 providing funding under the Stock Assessment Analytical Methods (SAAM) project to support
778 this research.
779

780 **References**

781 Benson, A.J., Cox, S.P., and Cleary, J.S. 2015. Evaluating the conservation risks of aggregate
782 harvest management in a spatially-structured herring fishery. Fish. Res. **167**: 101-113.
783 doi: 10.1016/j.fishres.2015.02.003

784 Beverton, R.J.H., and Holt, S.J. 1957. *On the dynamics of exploited fish populations*.
785 Fisheries Investment Series 2. 19. U.K. Ministry of Agriculture and Fisheries.
786 London: Chapman and Hall. 583 pp.

787 Bowler, D.E., and Benton, T.G. 2005. Causes and consequences of animal dispersal strategies:
788 relating individual behaviour to spatial dynamics. Biol. Rev. **80**: 205-225.

789 Bull, B., Francis, R.I.C.C., Dunn, A., McKenzie, A., Gilbert, D.J., Smith, M.H., Bain, R., and
790 Fu, D. 2012. CASAL (C++ algorithmic stock assessment laboratory): CASAL user
791 manual (v2.30). NIWA Tech. Rep. 135. 280 p.

792 Butterworth, D.S., and Punt, A.E. 1999. Experiences in the evaluation and implementation of
793 management procedures. ICES J. Mar. Sci. **56**: 985-998.

794 Cadrin, S.X, and Secor, D. 2009. Accounting for spatial population structure in stock
795 assessment: past, present, and future. *In* The future of fisheries science in North America.
796 *Edited by* R.J. Beamish and B.J. Rothschild. Springer Publishing. pp. 405-426. doi:
797 10.1007/978-1-4020-9210-7_22.

798 Carruthers, T.R., McAllister, M.K., and Taylor, N.G. 2011. Spatial surplus production
799 modeling of Atlantic tunas and billfish. Ecol. Appl. **21**: 2734-2755.

800 Ciannelli, L., Fisher, J.A.D., Skern-Mauritzen, M., Hunsicker, M.E., Hidalgo, M., Frank,
801 K.T., and Bailey, K.M. 2013. Mar. Ecol. Prog. Ser. **480**: 227-243.

802 Cope, J.M., and Punt, A.E. 2011. Reconciling stock assessment and management scales under
803 conditions of spatially varying catch histories. Fish. Res. **107**: 22–38. doi:
804 10.1016/j.fishres.2010.10.002.
805 de Moor, C.L., and Butterworth, D.S. 2015. Assessing the South African sardine resource: two
806 stocks rather than one? Afr. J. Marine Sci. **37**(1): 41-51.
807 Fahrig, L. 1993. Effect of fish movement and fleet spatial behaviour on management of fish
808 substocks. Nat. Resour. Model. **7**(1): 37-56.
809 Fournier, D.A., Hampton, J., and Sibert, J.R. 1998. MULTIFAN-CL: a length-based, age-
810 structured model for fisheries stock assessment, with application to South Pacific
811 albacore, *Thunnus alalunga*. Can. J. Fish. Aquat. Sci. **55**: 2105-2116.
812 Fournier, D.A., Skaug, H.J., Ancheta, J., Ianelli, J., Magnusson, A., Maunder, M.N., Nielsen, A.,
813 and Sibert, J. 2012. AD Model Builder: using automatic differentiation for statistical
814 inference of highly parameterized complex nonlinear models. Optim. Method. Softw. **27**:
815 233-249. doi: 10.1080/10556788.2011.597854.
816 Francis, R.I.C.C., and McKenzie, J.R. 2015. Assessment of the SNA1 stocks in 2013. New
817 Zealand Fisheries Assessment Report 2015/76. 82p.
818 Fu, C., and Fanning, L.P. 2004. Spatial considerations in the management of Atlantic cod off
819 Nova Scotia, Canada. N. Am. J. Fish. Manage. **24**: 775–784.
820 Geromont, H.F., and Butterworth, D.S. 2015. Complex assessments or simple management
821 procedures for efficient fisheries management: a comparative study. ICES J. Mar. Sci.
822 **72**(1): 262-274.

823 Goethel, D.R., Quinn, T.J., II, and Cadrin, S.X. 2011. Incorporating spatial structure in stock
824 assessment: movement modelling in marine fish population dynamics. Rev. Fish. Sci. **19**:
825 119–136. doi: 10.1080/10641262.2011.557451.
826 Goethel, D.R., Legault, C.M., and Cadrin, S.X. 2015. Testing the performance of a spatially
827 explicit tag-integrated stock assessment model of yellowtail flounder (*Limanda*
828 *ferruginea*) through simulation analysis. Can. J. Fish. Aquat. Sci. **72**(1): 164-177. doi:
829 10.1139/cjfas-2014-0244.
830 Goethel, D.R., Kerr, L.A., and Cadrin, S.X. 2016. Incorporating spatial population structure into
831 the assessment-management interface of marine resources. *In* Management science in
832 fisheries: an introduction to simulation-based methods. *Edited by* C.T.T. Edwards and
833 D.J. Dankel. Routledge, New York, NY. pp. 319-347.
834 Grandin, C.J., Hicks, A.C., Berger, A.M., Edwards, A.M., Taylor, N., Taylor, I.G., and Cox, S.
835 2016. Status of the Pacific Hake (whiting) stock in U.S. and Canadian waters in 2016.
836 Prepared by the Joint Technical Committee of the U.S. and Canada Pacific Hake/Whiting
837 Agreement, NMFS and FAO Canada. 165p.
838 Guan, W., Cao, J., Chen, Y., and Cieri, M. 2013. Impacts of population and fishery spatial
839 structures on fishery stock assessment. Can. J. Fish. Aquat. Sci. **70**:1178-1189.
840 Hampton, J., and Fournier, D.A. 2001. A spatially disaggregated, length-based, age-structured
841 population model of yellowfin tuna (*Thunnus albacares*) in the western and central
842 Pacific Ocean. Mar. Freshwater Res. **52**: 937-963.
843 Hanselman, D.H., Heifetz, J., Echave, K.B., and Dressel, S.C. 2015. Move it or lose it:
844 movement and mortality of sablefish tagged in Alaska. Can. J. Fish. Aquat. Sci. **72**: 238-
845 251.

Hart, D.R. 2001. Individual-based yield-per-recruit analysis, with an application to the Atlantic sea scallop *Placopecten magellanicus*. Can. J. Fish. Aquat. Sci. **58**: 2351–2358.

Hart, D.R. 2003. Yield- and biomass-per-recruit analysis for rotational fisheries, with an application to the Atlantic sea scallop (*Placopecten magellanicus*). Fish. Bull. **101**: 44-57.

Hilborn, R. 2002. The dark side of reference points. Bull. Mar. Sci. **70**(2): 403-408.

Hjort, J. 1914. Fluctuations in the great fisheries of northern Europe. Rapp. P.-v. Reun.-Cons. Int. Explor. Mer. **20**: 1–228.

Hoshino, E., Milner-Gulland, E.J., and Hillary, R.M. 2014. Why model assumptions matter for natural resource management: interactions between model structure and life histories in fishery models. J. Appl. Ecol. **51**: 632-641.

Karnauskas, M., Walter, J.F., and Paris, C.B. 2013. Use of the Connectivity Modeling System to estimate movements of red snapper (*Lutjanus campechanus*) recruits in the northern Gulf of Mexico. NOAA NMFS SEFSC. SEDAR31-AW10.

Kerr, L.A., Cadrin, S.X., and Secor, D.H. 2010a. Simulation modelling as a tool for examining the consequences of spatial structure and connectivity on local and regional population dynamics. ICES J. Mar. Sci. **67**: 1631–1639.

Kerr, L.A., Cadrin, S.X., and Secor, D.H. 2010b. The role of spatial dynamics in the stability, resilience, and productivity of an estuarine fish population. Ecol. Appl. **20**: 497–507.

Kerr, L.A., and Goethel, D.R. 2014. Simulation modelling as a tool for synthesis of stock identification information. *In* Stock identification methods: an overview. *Edited by* S.X.

868 Cadrin, L.A. Kerr, and S. Mariani. Elsevier Science and Technology, Burlington, MA.
869 pp. 501-533. doi: 10.1016/B978-0-12-397003-9.00021-7.
870 Kerr, L.A., Cadrin, S.X., and Kovach, A.I. 2014. Consequences of a mismatch between
871 biological and management units on our perception of Atlantic cod off New
872 England. ICES J. Mar. Sci. **71**(6): 1366-1381.
873 Kritzer, J.P., and Sale, P.F. 2004. Metapopulation ecology in the sea: from Levins' model to
874 marine ecology and fisheries science. Fish Fish. **5**: 131-140. doi: 10.1111/j.1467-
875 2979.2004.00131.x.
876 Kritzer, J.P., and Liu, O.W. 2014. Fishery management strategies for addressing complex spatial
877 structure in marine fish stocks. *In* Stock identification methods: an overview. *Edited by*
878 S.X. Cadrin, L.A. Kerr, and S. Mariani. Elsevier Science and Technology, Burlington,
879 MA. pp. 29-57.
880 Li, Y., Bence, J.R., and Brenden, T.O. 2015. An evaluation of alternative assessment approaches
881 for intermixing fish populations: a case study with Great Lakes lake whitefish. ICES. J.
882 Mar. Sci. **72**(1): 70-81. doi: 10.1093/icesjms/fsu057
883 Ling, S., and Milner-Gulland, E.J. 2008. When does spatial structure matter in models of wildlife
884 harvesting? J. Appl. Ecol. **45**: 63-71.
885 McGilliard, C.R., Punt, A.E., Methot, R.D., and Hilborn, R. 2015. Accounting for marine
886 reserves using spatial stock assessments. Can. J. Fish. Aquat. Sci. **72**: 262-280.
887 Mchich, R., Charouki, N., Auger, P., Raissi, N., and Ettahiri, O. 2006. Optimal spatial
888 distribution of the fishing effort in a multi fishing zone model. Ecol. Model. **197**:
889 274-280.

890 Methot, R.D., and Wetzel, C.R. 2013. Stock Synthesis: a biological and statistical framework for
891 fish stock assessment and fishery management. Fish. Res. **142**: 86-99. doi:
892 10.1016/j.fishres.2012.10.012.
893 Miller, T.J., and Andersen, P.K. 2008. A finite-state continuous-time approach for inferring
894 regional migration and mortality rates from archival tagging and conventional tag-
895 recovery experiments. Biometrics. **64**: 1196-1206.
896 Patterson, W.F. 2007. A review of movement in Gulf of Mexico red snapper: implications for
897 population structure. Am. Fish. Soc. Symp. **60**: 221-335.
898 Pelletier, D., and Mahévas, S. 2005. Spatially explicit fisheries simulation models for
899 policy evaluation. Fish and Fish. **6**: 307-349.
900 Pincin, J.S., and Wilberg, M.J. 2012. Surplus production model accuracy in populations
901 affected by a no-take marine protected area. Mar. Coast. Fish. **4**: 511-525.
902 Porch, C. 2003. VPA-2Box (ver. 3.01). Ass. Prog. Doc. ICCAT.
903 Porch, C., Kleiber, P., Turner, S. C., Sibert, J., Bailey, R. B., and Cort, J. L. 1998. The efficacy of
904 VPA models in the presence of complicated movement patterns. Collect. Vol. Sci. Pap.
905 ICCAT. **50**: 591-622.
906 Punt, A.E., and Cui, G. 2000. Including spatial structure when conducting yield-per-
907 recruit analysis. Australian society for fish biology workshop proceedings, pp.
908 176-182. September, 1999. Bendigo, Victoria, Australia.
909 Punt, A.E., and Methot, R.D. 2004. Effects of marine protected areas on the assessment
910 of marine fisheries. Am. Fish. Soc. Symp. **42**: 133-154.

911 Punt, A.E., Haddon, M., and Tuck, G.N. 2015. Which assessment configurations perform
912 best in the face of spatial heterogeneity in fishing mortality, growth, and
913 recruitment? A case study based on pink ling in Australia. Fish. Res. **168**: 85-99.
914 R Core Team. 2012. R: A language and environment for statistical computing. R
915 Foundation for Statistical Computing, Vienna, Austria. ISBN 3-900051- 07-0,
916 URL http://www.R-project.org/.
917 Reiss, H., Hoarau, G., Dickey-Collas, M., and Wolff, W.J. 2009. Genetic population structure of
918 marine fish: mismatch between biological and fisheries management units. Fish Fish.
919 **10**(4): 361–395.
920 Reuchlin-Hugenholtz, E., Shackell, N.L., and Hutchings, J.A. 2015. The potential for spatial
921 distribution indices to signal thresholds in marine fish biomass. PLoS ONE. **10**(3):
922 e0120500.
923 Reuchlin-Hugenholtz, E., Shackell, N.L., and Hutchings, J.A. 2016. Spatial reference points for
924 groundfish. ICES J. Mar. Sci. doi: 10.1093/icesjms/fsw123.
925 Rideout, R.M., and Tomkiewicz, J. 2011. Skipped spawning in fishes: more common than you
926 might think. Mar. Coast. Fish. **3**: 176-189.
927 Rooker, J.R., Secor, D.H., De Metrio, G., Schloesser, R., Block, B.A., and Neilson, J.D. 2008.
928 Natal homing and connectivity in Atlantic bluefin tuna populations. Science. **322**: 742-
929 744.
930 Sanchirico, J.N., and Wilen, J.E. 2001. Dynamics of spatial exploitation: a
931 metapopulation approach. Nat. Resour. Model. **14**(3): 391-418.

Sanchirico, J.N., and Wilen, J.E. 2005. Optimal spatial management of renewable resources: matching policy scope to ecosystem scale. J. Environ. Econ. Manag. **50**: 23-46.

SEDAR (Southeast Data, Assessment, and Review). 2015. Stock assessment of red snapper in the Gulf of Mexico 1872-2013—with provisional 2014 landings. Gulf of Mexico Science and Statistical Committee. Tampa, FL.

Sinclair, M. 1988. Marine populations: an essay on population regulation and speciation. University of Washington Press, Seattle, WA. 252pp.

Steneck, R.S., and Wilson, J.A. 2010. A fisheries play in an ecosystem theatre: challenges of managing ecological and social drivers of marine fisheries at multiple spatial scales. Bull. Mar. Sci. **86**(2): 387-411.

Takashina, N., and Mougi, A. 2015. Maximum sustainable yields from a spatially-explicit harvest model. J. Theor. Biol. **383**: 87-92. doi: 10.1016/j.jtbi.2015.07.028.

Thorson, J.T., Fonner, R., Haltuch, M.A., Ono, K., and Winker, H. 2016. Accounting for spatio-temporal variation and fisher targeting when estimating abundance from multispecies fishery data. Can. J. Fish. Aquat. Sci. doi: 10.1139/cjfas-2015-0598.

Truesdell, S.B., Hart, D.B., and Chen, Y. 2016. Effects of spatial heterogeneity in growth and fishing effort on yield-per-recruit models: an application to the US Atlantic sea scallop fishery. ICES J. Mar. Sci. **73**(4): 1062-1073.

Tuck, G.N., and Possingham, H.P. 1994. Optimal harvesting strategies for a metapopulation. Bull. Math. Biol. **56**: 107-127.

Turchin, P. 1998. Quantitative analysis of movement: measuring and modelling population redistribution in animals and plants. Sinauer Associates, Inc., Sunderland, MA, USA.

955 Wilberg, M.J., Irwin, B.J., Jones, M.L., and Bence, J.R. 2008. Effects of source-sink dynamics
956 on harvest policy performance for yellow perch in southern Lake Michigan. Fish. Res.
957 **94**: 282-289.
958 Wilen, J.E. 2004. Spatial management of fisheries. Mar. Resour. Econ. 19: 7-19.
959 Ying, Y., Chen, Y., Lin, L., and Gao, T. 2011. Risks of ignoring fish population spatial structure
960 in fisheries management. Can. J. Fish. Aquat. Sci. **68**: 2101–2120. doi: 10.1139/f2011-
961 116.

962
963

964 **Tables**

965 **Table 1:** Glossary of terms used throughout the article.

966

Term	Definition
Spatial Population Structure	The spatiotemporal distribution of a resource resulting from environmental or ecosystem interactions (i.e., connectivity) and reproductive dynamics.
Connectivity	Movement of individuals among geographic areas at any life stage (e.g., larval or adult).
Area	A geographic unit representing the spatial extent over which a homogenous fishing mortality acts. Depending on the type of population structure, an area may contain a segment of a single population, an entire population or segments of multiple populations.
Population	A self-reproducing biological entity within which all fish are able to reproductively mix resulting in a single SSB that determines population-specific recruitment values based on a unique stock-recruit function.
System-wide	The entire spatial domain of the model.
Panmictic	A single, unit population with no spatial heterogeneity.
Single Population with Spatial Heterogeneity	A single population with abundance distributed over multiple areas.
Metapopulation	A network of populations each with unique stock-recruit relationships, but which can reproductively mix. It is assumed that environmental factors drive demographic rates.
Natal Homing	A population structure wherein multiple populations overlap spatially, but do not reproductively mix. Fish always retain the life history characteristics of their natal population, which assumes that genetics drive demographic parameters.
Unidirectional Movement	Movement among areas is only allowed in one direction (e.g., source-sink dynamics).
Bidirectional Movement	Movement is allowed among all areas.
Spawning Migration	An instantaneous migration at the time of spawning that allows a fish to reside outside of its natal area throughout the year, but still add to the SSB of its natal population.
Natal Return	A return migration at a specific age (i.e., a_{RET}) that emulates an ontogenetic migration.
Harvest Rate	The fraction of the biomass that is harvested within a given area (i.e., yield/biomass).

967

968

969

970

971

972

973

974

975

976 **Table 2:** Input parameters for a midwater pelagic, hake-like species used to evaluate *BRP_Dev*
977 and *HL_App* models. Abundance and recruitment are in 1000s of fish, weight is in kg,
978 and SSB is in metric tons.
979

Age	Selectivity	Maturity	Initial Abundance	M	Weight
1	0.00	0.00	3,125,000	0.226	0.101
2	0.12	0.12	2,538,636	0.226	0.273
3	0.54	0.54	2,062,295	0.226	0.377
4	0.71	0.71	1,675,333	0.226	0.473
5	0.87	0.87	1,360,979	0.226	0.545
6	1.00	1.00	1,105,610	0.226	0.622
7	1.00	1.00	898,157	0.226	0.674
8	1.00	1.00	729,630	0.226	0.754
9	1.00	1.00	592,725	0.226	0.805
10	1.00	1.00	481,508	0.226	0.833
11	1.00	1.00	391,159	0.226	0.909
12	1.00	1.00	317,764	0.226	0.952
13	1.00	1.00	258,139	0.226	0.938
14	1.00	1.00	209,703	0.226	0.918
15+	1.00	1.00	170,355	0.226	0.982
R_0	3,125,000	SSB_0	2,397,000	Steepness	0.814

980

981 **Table 3:** Scenario list for the *Move+Prod* subset of *BRP_Dev* models. For natal return and
982 spawning migration models, adult residency actually corresponds to the rate of return.
983 'All' indicates 100% residency, 'high' means the high residency values are used, and
984 'low' signifies that the low residency values are used. For unidirectional movement,
985 100% residency is implied for the sink (area 1).
986

Scenario	Population Structure	Residency Level		Movement Type				
		Adult	Larval	None	Unidirectional	Bidirectional	Spawning Migration	Natal Return
1	1 Population, Panmictic	all	all	x				
2	1 Population, 2 Areas	all	all	x				
3	1 Population, 2 Areas	high	low		x			
4	1 Population, 2 Areas	low	high		x			
5	1 Population, 2 Areas	high	high		x			
6	1 Population, 2 Areas	low	low		x			
7	1 Population, 2 Areas	high	low			x		
8	1 Population, 2 Areas	low	high			x		
9	1 Population, 2 Areas	high	high			x		
10	1 Population, 2 Areas	low	low			x		
11	Metapopulation	all	all	x				
12	Metapopulation	high	low		x			
13	Metapopulation	low	high		x			
14	Metapopulation	high	high		x			
15	Metapopulation	low	low		x			
16	Metapopulation	high	low			x		
17	Metapopulation	low	high			x		
18	Metapopulation	high	high			x		
19	Metapopulation	low	low			x		
20	Natal Homing	high	low		x		x	
21	Natal Homing	low	high		x		x	
22	Natal Homing	high	high		x		x	
23	Natal Homing	low	low		x		x	
24	Natal Homing	high	low		x			
25	Natal Homing	low	high		x			
26	Natal Homing	high	high		x			
27	Natal Homing	low	low		x			
28	Natal Homing	high	low			x	x	
29	Natal Homing	low	high			x	x	
30	Natal Homing	high	high			x	x	
31	Natal Homing	low	low			x	x	
32	Natal Homing	high	low			x		
33	Natal Homing	low	high			x		
34	Natal Homing	high	high			x		
35	Natal Homing	low	low			x		
36	Natal Homing	high	low		x			x
37	Natal Homing	low	high		x			x
38	Natal Homing	high	high		x			x
39	Natal Homing	low	low		x			x
40	Natal Homing	high	low			x		x
41	Natal Homing	low	high			x		x
42	Natal Homing	high	high			x		x
43	Natal Homing	low	low			x		x

987

988 **Table 4:** Qualitative summary of *BRP_Dev* results describing the relative value of each factor
989 (SSB, yield, and harvest rate) for various population structures and movement types.
990 Results are averaged across movement levels within each movement type to provide
991 an overview of results. Qualitative values (low, medium or high) represent relative
992 comparisons for that factor across population structure and movement types within
993 that geographic area (i.e., system-wide or area-specific).

994

Population Structure	Movement Type	Factor	System-Wide	Area 1	Area 2
1 Population, Panmictic	No Movement	SSB	High	-	-
		Yield	High	-	-
		uMSY	Moderate	-	-
1 Population, 2 Areas	Unidirectional	SSB	High	High	Low
		Yield	High	High	Low
		uMSY	Moderate	Moderate/High	Moderate/Low
	Bidirectional	SSB	High	Moderate/High	Moderate
		Yield	High	Moderate	Moderate
		uMSY	Moderate	Moderate	Moderate
Metapopulation	Unidirectional	SSB	Moderate/Low	Moderate	Moderate/Low
		Yield	Moderate/Low	High	Low
		uMSY	Moderate/High	High	Low
	Bidirectional	SSB	High	Moderate	Moderate/High
		Yield	High	Moderate/High	Moderate/Low
		uMSY	Moderate	High	Moderate/Low
Natal Homing	Unidirectional, Spawning Migration	SSB	High	Moderate/Low	Moderate/High
		Yield	High	Moderate/Low	Moderate
		uMSY	Moderate	Moderate/Low	Moderate/High
	Bidirectional, Spawning Migration	SSB	High	Moderate/Low	Moderate/High
		Yield	High	Low	Moderate/High
		uMSY	Moderate	Moderate/Low	Moderate/High
	Unidirectional, Natal Return	SSB	Moderate	Moderate/Low	Moderate/High
		Yield	Moderate	Low	Moderate
		uMSY	Moderate	Moderate/Low	Moderate/High
	Bidirectional, Natal Return	SSB	Moderate	Moderate/Low	Moderate/High
		Yield	Moderate	Low	Moderate/high
		uMSY	Moderate	Low	Moderate/High

995

Table 5: Qualitative summary of *HL_App* results describing the relative rate of occurrence (compared to results of other spatial structure scenarios) for each factor (i.e., depletion, foregone yield or underutilization) and each of the true and assumed population structure combinations. Results are averaged across movement types and geographic areas within any given assumed to true population structure comparison in order to provide a qualitative overview of results. When true and assumed spatial structures are identical, results compare different movement assumptions (e.g., unidirectional versus bidirectional movement) for the given population structure.

Assumed Population Structure	Factor	True Population Structure: 1 Population, Panmictic	1 Population, 2 Areas	Metapopulation	Natal Homing
1 Population, Panmictic	Depletion	-	Moderate	Moderate/High	Low
	Foregone Yield	-	Low	High	Low
	Underutilization	-	Low	High	Low
1 Population, 2 Areas	Depletion	Low	Low	Moderate	Low
	Foregone Yield	Low	Low	Moderate	Low
	Underutilization	Low	Low	High	Low
Metapopulation	Depletion	Low	Moderate/High	Moderate	High
	Foregone Yield	Low	High	High	Moderate
	Underutilization	Low	High	Moderate	High
Natal Homing	Depletion	Low	Low/Moderate	Moderate	Low
	Foregone Yield	Low	Low	Moderate	Low
	Underutilization	Low	Low	High	Low

Figures

Figure 1: Outline of the two-stage generalized simulation model. MSY-based BRPs were chosen for illustrative purposes, but other depletion or yield-based management benchmarks could be defined. Similarly, u_{MSY} in stage 2 could be replaced with any input harvest rate or yield level. Stages were run independently.

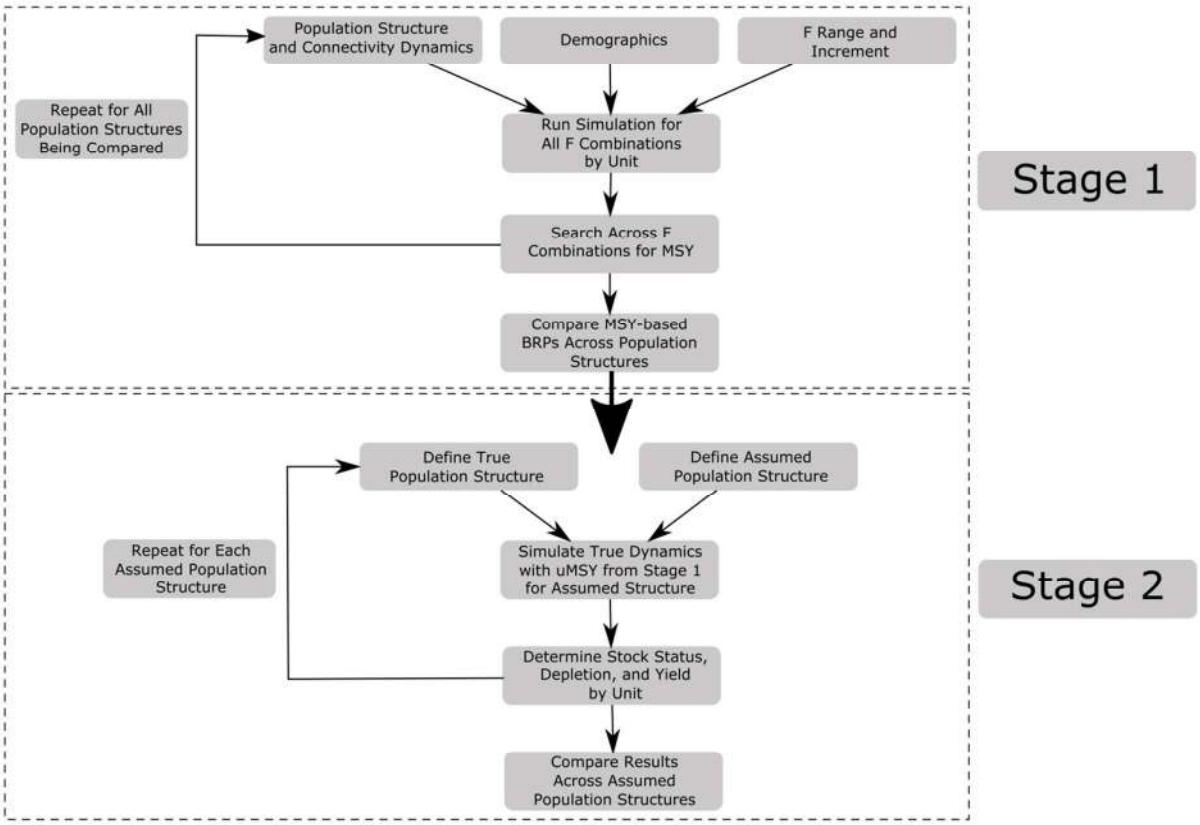

1014 **Figure 2:** Spatial (A) and spatiotemporal (B) dynamics of the simulation model (see Equations
1015 1-5 and associated text for a description of terms). Large circles represent geographic
1016 areas within which multiple populations can mix (for spatial heterogeneity smaller
1017 circles represent areas within a single population). Mixing (dark overlap regions) is
1018 depicted as taking place in partial areas for illustrative purposes, but actually takes
1019 place across the extent of the given geographic area. Dotted lines illustrate
1020 movement, while narrow solid lines represent recruitment. The small circles in the
1021 bottom panel (B) represent the segment of a population (population is denoted by the
1022 subscript) outside its natal area, which overlaps with the natal population of the
1023 geographic area (large circles; area is represented by the superscript).
1024

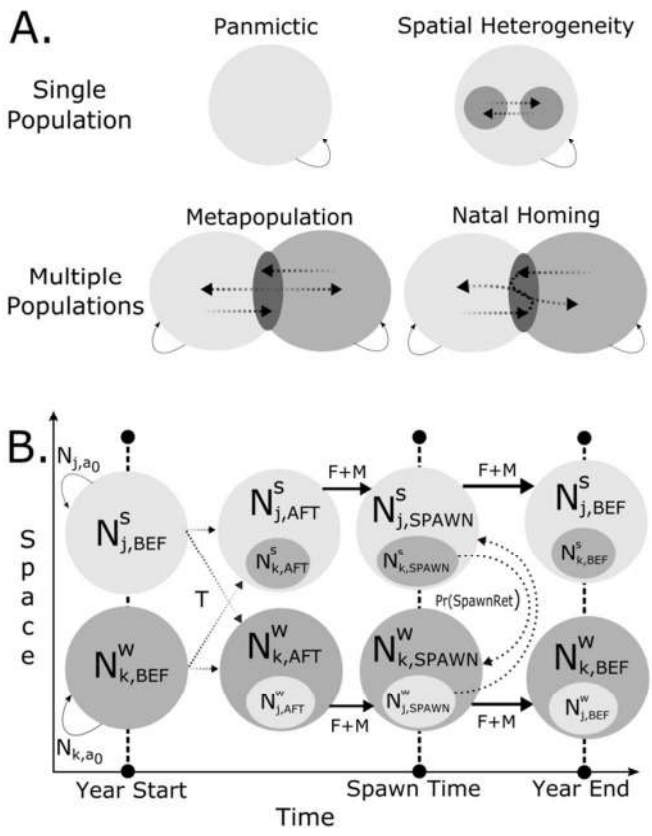

1025

1026 **Figure 3:** Results from the *Move+Prod* subset of *BRP_Dev* models illustrating MSY-based
1027 reference points. MSY and SSB_{MSY} are in 1000s of metric tons, while u_{MSY} is the
1028 harvest rate (yield/biomass). Scenarios are grouped by the general type of spatial
1029 population structure used in the simulation model (specifics of each scenario are
1030 shown in Table 3). Values are provided by area and system-wide (i.e., total summed
1031 across areas).

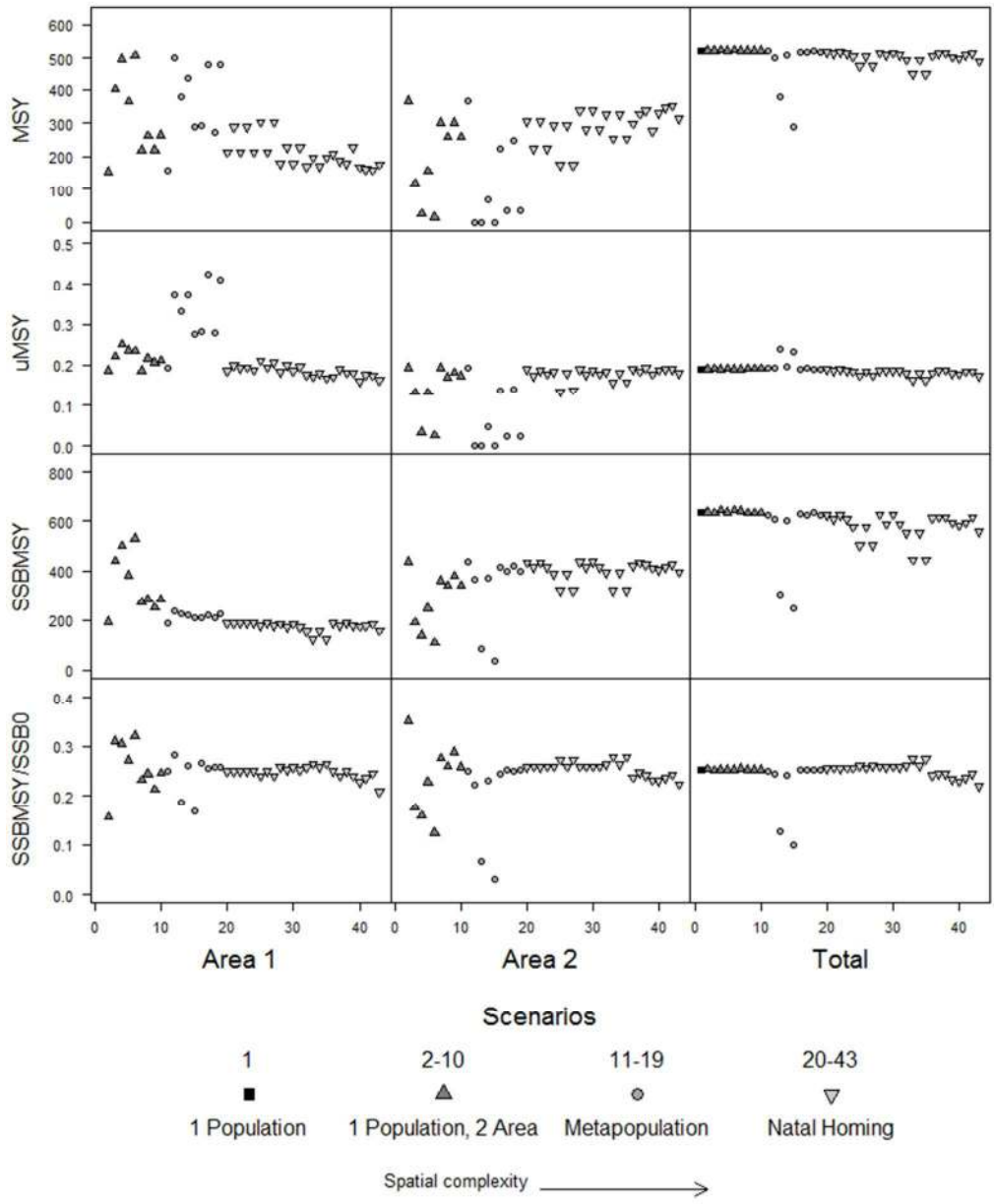

1032

1033 **Figure 4:** Results from *HL_App* models demonstrating stock status relative to the true SSB_{MSY}
1034 (i.e., $SSB_{Terminal}/SSB_{MSYTrue}$) assuming panmictic population structure. The true
1035 spatial population structure for each scenario is described by the x-axis tabular labels.
1036 Values are provided by area and system-wide (i.e., total summed across areas).
1037

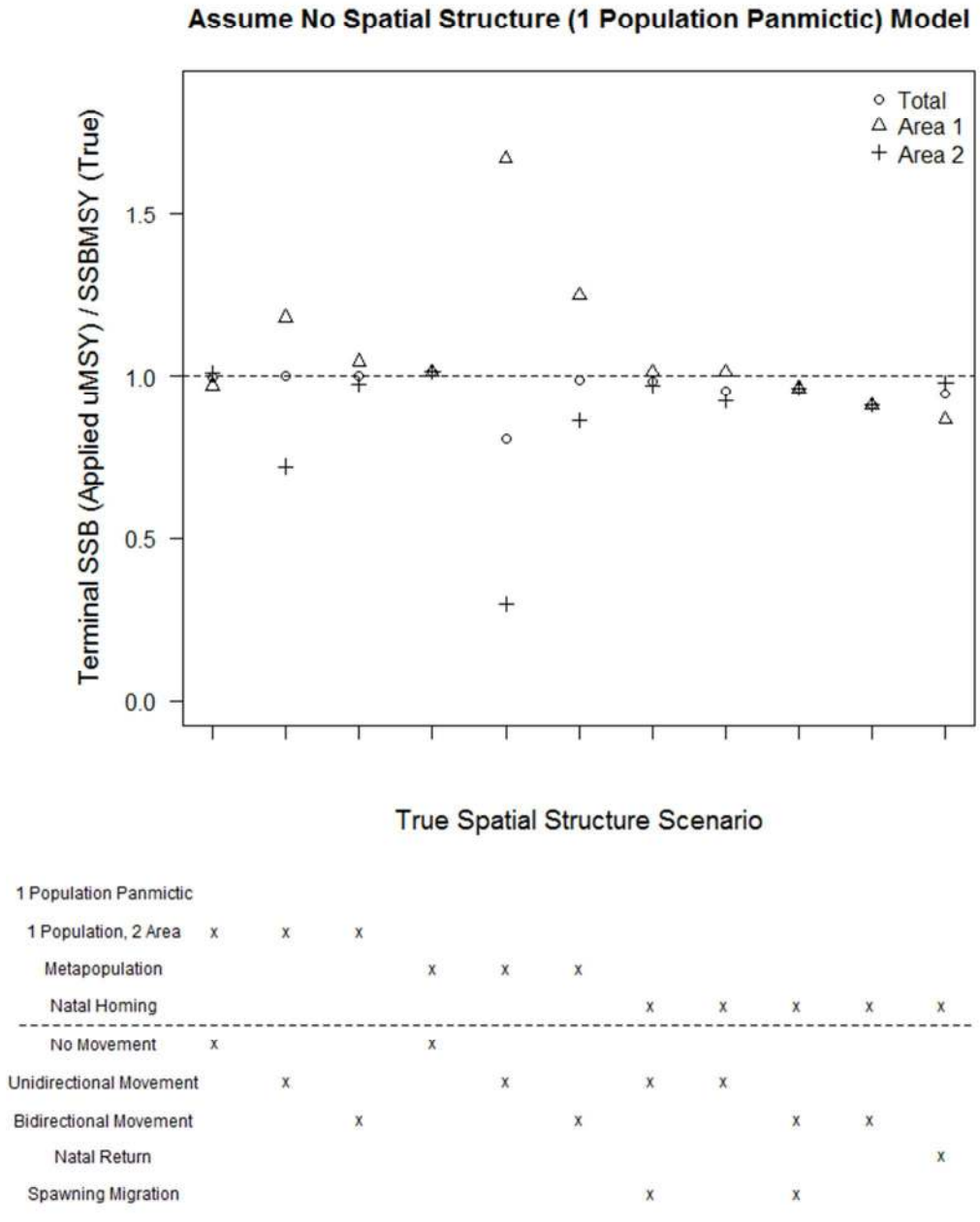

1038

1039 **Figure 5:** Results from *HL_App* models demonstrating stock status relative to the true SSB_{MSY}
1040 (i.e., $SSB_{Terminal}/SSB_{MSYTrue}$) assuming metapopulation structure with source-sink
1041 dynamics (i.e., unidirectional movement; left panel) and bidirectional movement
1042 (right panel). The true spatial population structure for each scenario is described by
1043 the x-axis tabular labels. Values are provided by area and system-wide (i.e., total
1044 summed across areas).
1045

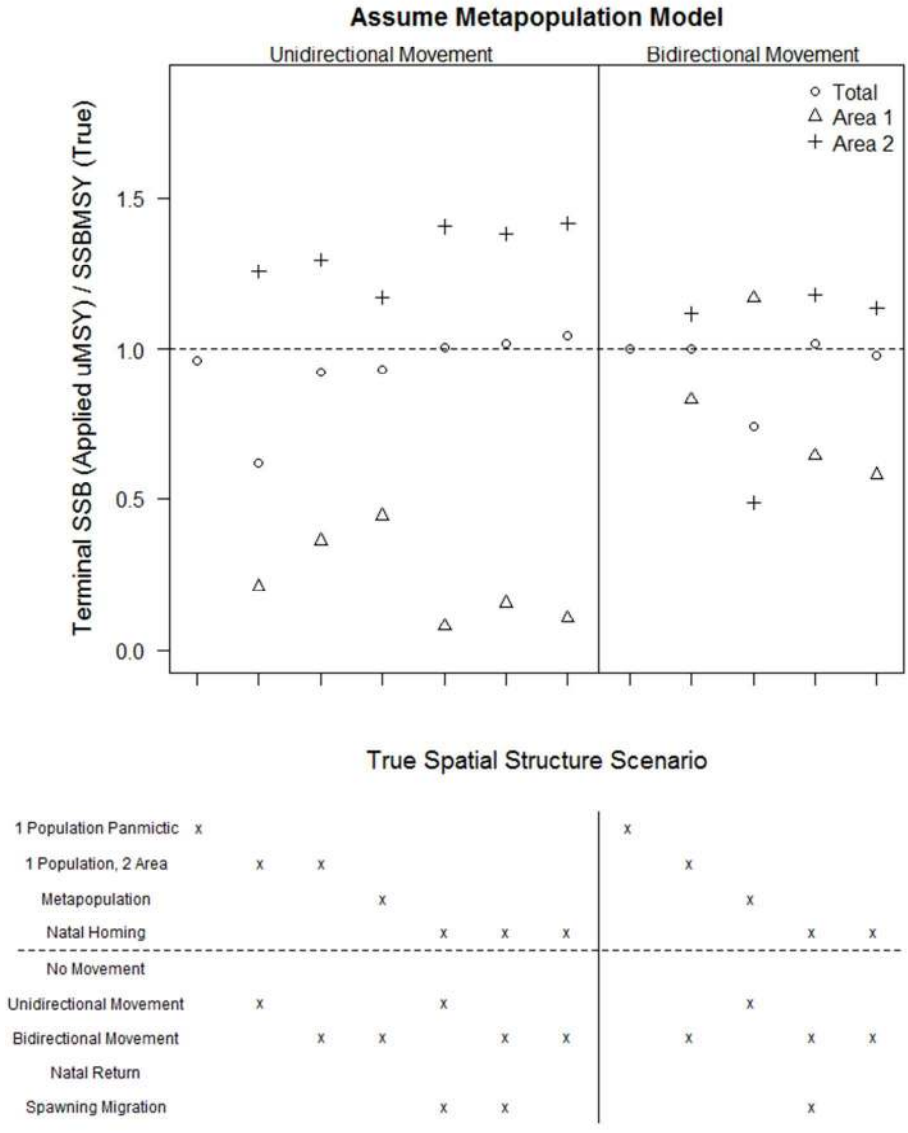

1046

1047 **Figure 6:** Results from *HL_App* models demonstrating stock status relative to the true SSB_{MSY}
1048 (i.e., $SSB_{Terminal}/SSB_{MSYTrue}$) assuming natal homing population structure. The left
1049 hand panel illustrates results assuming bidirectional movement and spawning
1050 migrations (except the last two scenarios, which assume no spawning migration),
1051 while the right hand panel displays results assuming natal return. The true spatial
1052 population structure for each scenario is described by the x-axis tabular labels.
1053 Values are provided by area and system-wide (i.e., total summed across areas).
1054

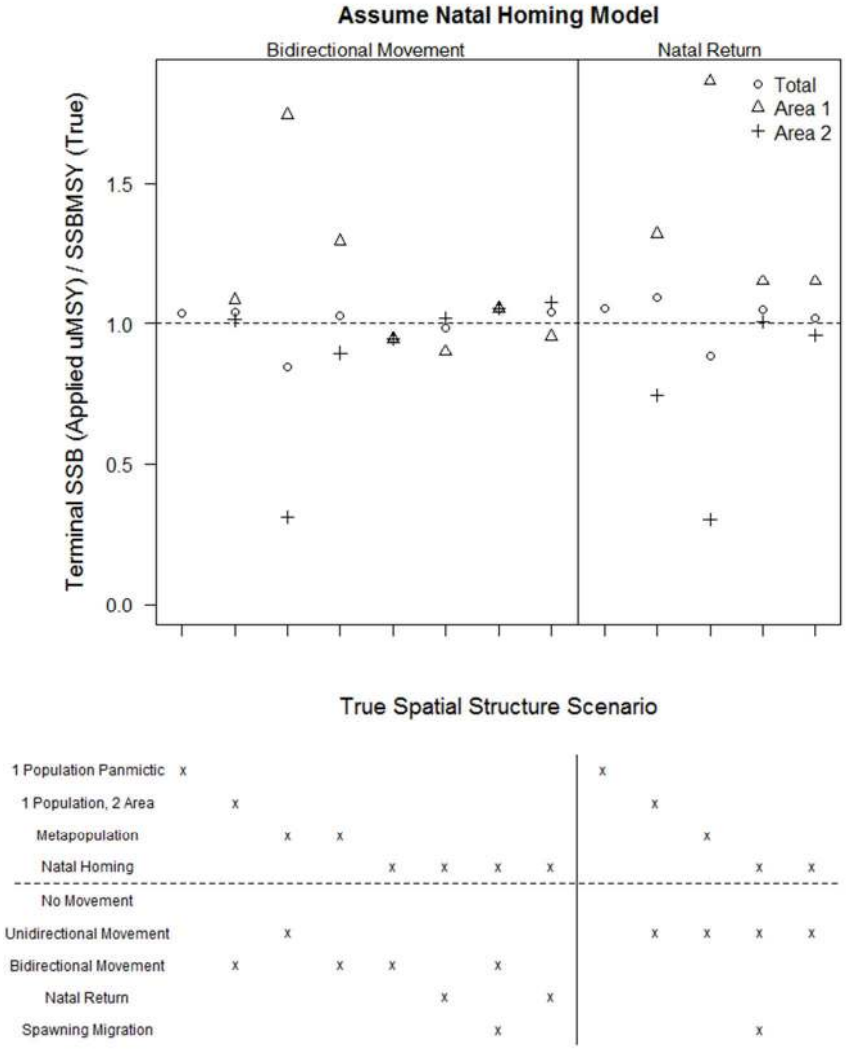

1055

Figure 7: Results from *Snapper_Uneven_Eff* scenarios demonstrating stock status relative to the true SSB_{MSY} (i.e., $SSB_{Terminal}/SSB_{MSYTrue}$) assuming panmictic stock structure and allowing a nonhomogeneous distribution of effort (i.e., harvest rate in area 1 is halved and harvest rate in area 2 is increased until the total system-wide harvest rate reaches the desired panmictic u_{MSY}). The true spatial population structure for each scenario is described by the x-axis tabular labels, where an asterisk represents the lowest residency rate (i.e., 80%) scenario. Values are provided by area and system-wide (i.e., total summed across areas).